N91-10503

Structures Observed on the Spot Radiance Fields During the FIRE Experiment

Genevieve Seze*, Leonard Smith** and Michel Desbois*
*LMD/Ecole Polytechnique 91128 Palaiseau Cedex (France)
**DAMTP, Cambridge University (UK)

Introduction

Three Spot images taken during the FIRE experiment on stratocumulus (july 1987) have been analysed. From this high resolution data detailed observations of the true cloud radiance field may be made. The structure and inhomogeneity of these radiance fields hold important implications for the radiation budget, while the fine scale structure in radiance field provides information on cloud dynamics. Wieliki and Welsh (1986) and Parker et al. (1986) have quantified the inhomogeneities of the cumulus clouds through a careful examination of the distribution of cloud (and hole) size as functions of an effective cloud diameter and radiance threshold. Cahalan (1988) has compared for different cloud types (stratocumulus, fair wheather cumulus, convective clouds in the ITCZ) the distributions of clouds (and holes) sizes, the relation between the size and the perimeter of these clouds (and holes), and examining the possibility of scale invariance. We extended these results from Landsat resolution (57m and 30m) to the Spot resolution (10m) resolution in the case of boundary layer clouds. Particular emphasis is placed on the statistics of zones of high and low reflectivity as a function of a threshold reflectivity.

Data

Each Spot instrument returns one panchromatic images (10m resolution) and three multispectral images (20m resolution). These images are obtained from the measure of solare enery in a large spectral band (0.51-0.73) and three narrower bands at visible and infrared wavelengths. The saturation is reached in the panchromatique band for 30% of reflectivity and in the multispectral bands respectively for 50%, 60% and 80% of reflectivity. Data are discretized in digital count comprised between 0 and 255. In the panchromatic image the sea reflectivity corresponds to about 25 counts.

Three different Spot scenes have been recorded during the FIRE experiment: One 60km by 80km scene on the 7th of july both in panchromatic mode and multispectral mode, one double scene of 120km by 120km on the 8th of july in panchromatic mode and on 60km by 66km scene on the 19th both in panchromatic and multispectral mode. The 7th and 8th are very cloudy. However, inspite of the small variability in radiances, different structures appear. The scene for the 19th of july is on the opposite characterized by the presence of very small clouds. From these data sets, three regions of 1024 by 1024 pixels (10km by 10km) have been extracted (Fig. 1). The first region is composed of a mixing of high reflectivity and low reflectivity structures. The second region has increasing reflectivity from the center to the edges. Scene 3 is a almost clear sky with sparse small clouds of various size but low reflectivity.

Radiance field analysis

For each of the three scenes, binary images have been constructed in order to study the size distribution of the high reflectivity and low reflectivity regions and their spatial dispersion. The images are constructed by using radiance threshold; for a certain threshold R, pixels having a radiance larger than R in the original image, are assigned the value 1 in the binary image while the other pixels are assigned the value 0. The pixels with value 1 will be called high reflectivity pixels or "bright" pixels, whereas pixels with value 0 will be called low reflectivity pixels or "dark" pixels. The fraction of pixels in each state will vary with the chosen threshold; for scene 1 and scene 2, thresholds have been chosen so as to obtain a "dark" ("bright") pixel percentage : 10%, 30%, 50%, 70%, 90%. For the clear scene on the 19th (scene 3), more

C-4

than 93% of the pixels are clear sky. In this case, four thresholds have been chosen as to have 93%, 95%, 97%, 98% of the pixels darker than the threshold.

As the radiance threshold is increased the binary images of the first scene more and more resembles an open cell or cumulus cloud field. In binary images of scene 2, the interior hole becomes sucessively better defined, the similarity with an open cell is enhanced. For images of the third scene, the effect of increasing the threshold is first to mask noise over the sea, then to decrease the cloud surface area. For each threshold-related binary image, the number of "dark" and "bright" regions have been determined; then for each of these regions various parameters have been computed. We will concentrate only on two of them: the surface area or the number of pixels forming the region and the so called "perimeter" or the number of pixel edges which are at boundary between a "dark" and a "bright" pixel. From the surface area an equivalent diameter has been computed (see Wieliki and Welsh, 1986). To study their distributions the "dark" ("bright") surface areas have been gathered in classes of equal step of ln(2) in ln(D). Boundary between class increase by factor of 2 (10m, 20m, 40m ...) Figure 2 show these distributions for scene 2 and the 5 thresholds on a log/log plot.

For scene 1 and 2, the observed dependence in the number of regions, and the distribution of the surface area of these regions versus thresholds indicates that as the percentage of "bright"("dark") pixels increases, the number of areas increases first and then decreases; at first as the "bright" ("dark") pixel percentage increases the number of new regions which appear is larger than the number of regions which are gathered, then the reverse situation occurs. The magnitude of these increases and decreases and the percentage value for the break point are related to the spatial organisation of the bright and dark areas. For a given percentage, the number of small "dark" regions (10m to 160m in equivalent diameter) is larger than the number of small "bright" regions. Especially, the darkest pixels are wider spread in small regions than the brightest pixels. For scene 1 the number of "bright"("dark") regions for a certain percentage is higher than for scene 2; the spatial mixing of the "bright" and "dark" regions of various area surface is larger in scene 1.

For a given percentage of "bright" ("dark") pixels, the number of region decrease versus surface area increase is obvious; this increase is relatively uniform on the log/log plot (Fig. 2) for surface area larger than 10m and smaller than 1280m. Exceptions are 90% cases of "bright"/"dark" regions, the number of regions and specially of small regions consequently decreases. The relatilly uniform decrease observed, is in agreement with previous results found by Cahalan (1988) for Landsat cloudy scenes; these results show that distributions of surface areas of clouds (or holes) often decrease versus surface area increase as a power law; the exponent is related to the cloud field beiing studied. This exponent is defined as the area exponents by Lovejoy and Shwertzer (1988). For boundary layer clouds, Cahalan finds an exponent value of 1.5 for low thresholds, and observes an increase of this exponent for increasing thresholds. In the present study, when the power law aproximation seems reasonable (a percentage of pixels smaller than 90% and generally surface areas between 20m and 1240m), the exponent value found ranges between 1. and 1.3.

The length of the boundary has also been computed, it appears that in the case of a small threshold the number of boundary pixel is larger than in the case of a high threshold, because of the larger spatial dispersion of the darkest pixels as compared to the brightest pixels. In order to have a measure of the complexity of the boundary of these "bright" ("dark") regions, we have plotted for each region its perimeter value versus the root mean square of its surface area on a log/log scale. The same linear relationship as found by Lovejoy (1982) on Goes images and by Cahalan (1988) on Lansat appears on these graphs; the fitted slope is close to 1.3.

For scene 3 the number of "bright" or "cloud" regions is small, and the diameter of these clouds is generally between 10m and 360m. The large decrease of the number of regions (1135 to 562) occurs for thresholds between 29 and 31 which only correspond to about 0.4% reflectivity difference. This decrease is due to the disparition of

noisy sea pixels. As for scene 1 and 2 the decrease of the distribution slope with surface area increase (for surface area between 20m and 320m) is relatively uniform. The slopes observed range between -.8 and -.7.

On the other hand, a box counting technic on a regular grid has been used to study the spatial distribution of these "bright" ("dark") regions. Box counting technics have been developped as a way to estimate the dimension of fractal sets (Lovejoy and Shertzer, 1988). It has also been used to study the effect of sensor resolution (Shenk and Salomonson 1972). To apply this technic, different resolution grids are defined, for resolution elements varying from a quarter of the image (lowest resolution), to one pixel (highest resolution) and dividing at each step the resolution element by 4; then for each resolution the percentage of "bright" ("dark") coverage is determined by counting the number of resolution elements containning at least one "bright" ("dark") pixel. For each scene and each threshold, the percentages of "bright" and "dark" coverages in function of the resolution (Eps) have been plotted. For each curve several parameters have been extracted. The first parameter is the exponent d0 which for a fractal set equal its dimension. d0 is obtained by fitting a a power law (M(Eps)=Eps**d0) through the scatter. The other parameters M0, Beta and A are obtained by fitting a function F (F=M0+A*Eps**Beta). F is an empirical scaling law to determine the "true area" of assumed "fat fractal" set (Farmer and Umberger, 1985; Smith, 1986).

These different parameters vary in function of the increase of the "bright" ("dark") pixel percentage and of the scene studied. They are related to the surface area distribution of the "bright" and "dark" regions and to their relative spatial disposition. For high percentages, d0 is close to 2, the fractal dimension of an area being 2. However as the percentage of "bright" ("dark") pixels decreases d0 decreases due to the region increasing scatter. Correlatively, A and Beta increase. For a given percentage of "dark" and "bright" pixels, the value of d0 for "dark" regions is smaller than for "bright" regions, especially for the lowest percentages (1.5 and 1.7); On the opposite A and Beta are larger in the case of "dark" regions. These differences between the "dark" and "bright" cases are related to the larger number of regions found for the darkest image than for the brightest image. Differences are observed between scene 1 and scene 2 in these parameter values and are related to the spatial organisation of the "bright" and "dark" region in these regions; especially, the differences between the parameters associated to the "dark" areas and to the "bright" areas are larger for scene 1 than scene 2.

Conclusion

Some results found are in agreement with previous studies on satellite high resolution data; the number of "bright" and "dark" region decrease versus surface area increase can be in some cases aproximated by a power law; the perimeter and the surface area are found to be a power law related with an exponent close to 1.3. However, our study focussed, at least for two of the scenes, on the change in the scales of variability versus the percentage of pixels declared "thick" ("thin"). This shows the possibility for differentiating spatial structures in an apparently homogeneous cloud field. The parameters obtained from the fat fractal scaling can give usefull indications on these structures, and allow to aproximate the error in cloud cover estimation from coarse resolution data; further studies must be pursued to check the conditions for which fat fractal scaling can be applied to the cloud radiance field. The third scene shows the existence of very small and low refectivity clouds and the importance of noise in the data for the choice of a cloud/no cloud detection threshold. This study has to be continued on more scenes; the comparison between the 10m and 20m resolution images has to be developped and simultaneously the effect of a spatial sampling or averaging of the data must be tested. Comparison of these 60km by 60km Spot scenes with the corresponding 1km resolution Goes radiance field has to be done.

References

R. F. Cahalan, 1988: Landsat observations of fractal cloud structure. Non Linear Variability in Geophysics. S.L Eds, Reidel.

D.K. Umberger and Farmer J.D. , 1985: Fat fractals on the enery of surface. Phys. Rev. Lett. 55, 661-664.

S. Lovejoy, 1982: Area-perimeter relation for rain and cloud areas. Science, 26, 185-187.

S. Lovejoy and Shertzer D., 1988: Multifractal analysis techniques and geophysical applications. Non Linear Variability in Geophysics. S.L Eds, Reidel.

L. Parker, Welsh R.M. and Musil D.J., 1986: Analysis of spatial inhomogeneities in cumulus clouds using high spatial resolution Lansat data. J. Climate Appl. Meteor., 25, 1301-1314.

William E. Shenk and Salomonson V. V., 1972: A simulation study exploring the effects of sensor spatial resolution on estimates of cloud cover from satellites. J. Appl. Meteor., 11, 214-220.

L. Smith, 1986: Fat fractal scaling of cloud areas. Conference on Nonlinear Variability in Geophysics. 25-29 august 1986. McGill University, Montreal.

Bruce Wieliki and Welch R. W., 1986: Cumulus cloud properties using Landsat satellite data. J. Climate Appl. Meteor., 25, 261-276.

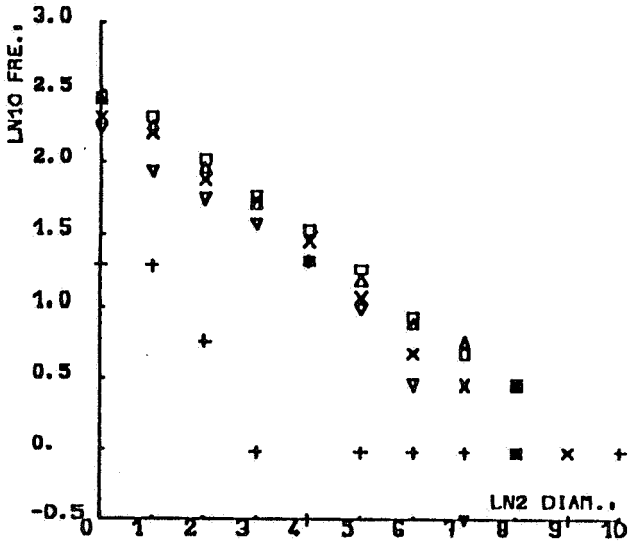

Figure 2: Distributions of the surface areas of the "thick" regions in scene 2 for 5 thresholds; the , , , , , correspond to thresholds 10%,30%,50%,70%,90%.

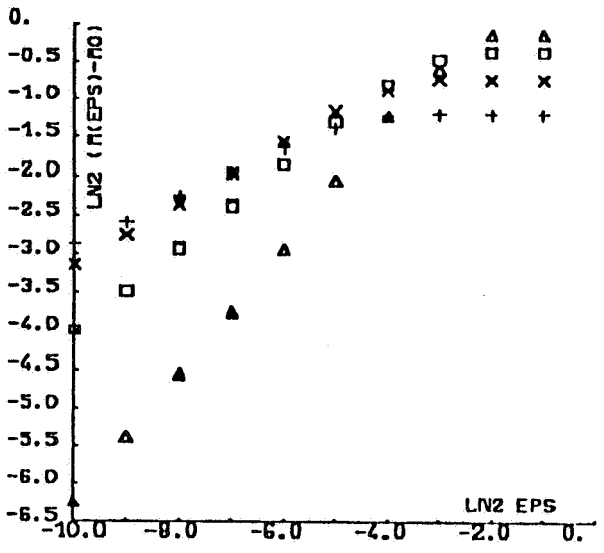

Figure 3: For scene 1, difference of the "thick" pixel percentage (M(Eps)) with the estimated percentage M(0) versus resolution Eps for 4 thresholds; the , , , , , correspond to thresholds 10%/30%/50%/70%.

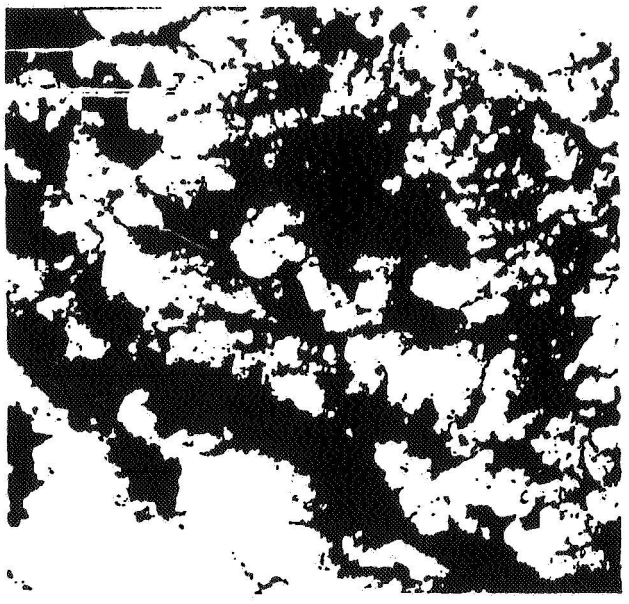

a) 2048 by 2048 pixel square centered on region 1; the black (white) represents the radiance 100 (255).

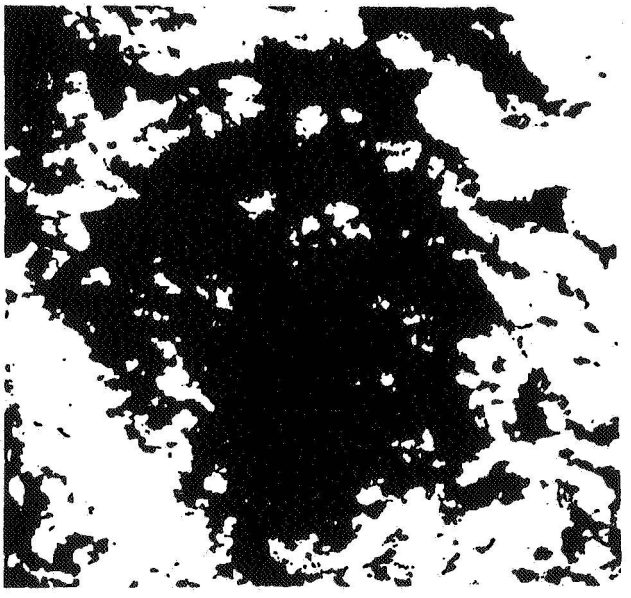

b) 1024*1024 pixel square corresponding to region 2; the black (white) represents the radiance 60 (255).

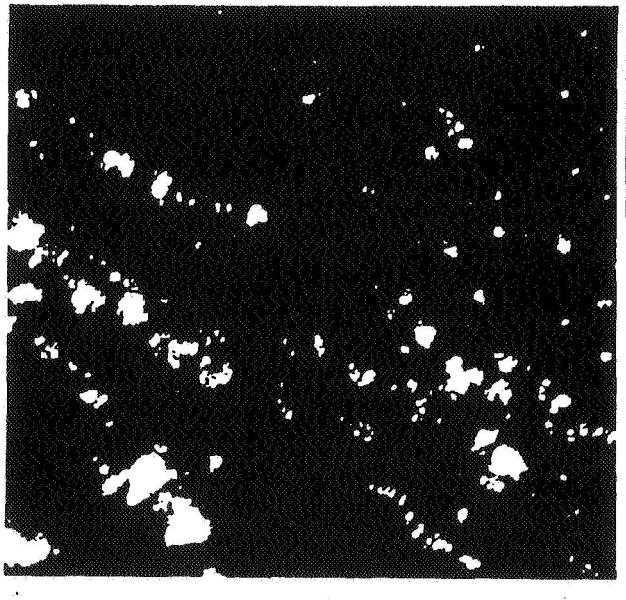

c) 2048 by 2048 pixel square; region 3 is a 1024 by 1024 pixel square placed on the middle left part of the scene. the black (white) represents the radiance 25 (80).

Figure 1: Spot panchromatique images.